arXiv:1510.01418v1 [physics.atom-ph] 6 Oct 2015

Inelastic processes in Na^+-Ne, Ar and Ne^+, Ar^+-Na collisions in energy range $0.5-14$ keV

R. A. Lomsadze[1], M. R. Gochitashvili[1], R. Ya. Kezerashvili[2,3]
[1] *Tbilisi State University, Tbilisi, 0128, Georgia*
[2] *New York City College of Technology, The City University of New York, Brooklyn, NY 11201, USA*
[3] *The Graduate School and University Center, The City University of New York, New York, NY 10016, USA*
(Dated: October 7, 2015)

Absolute cross sections for charge-exchange, ionization and excitation in Na^+-Ne and Na^+-Ar collisions were measured in the ion energy range $0.5-10$ keV using a refined version of a capacitor method, and collision and optical spectroscopy methods simultaneously in the same experimental set-up. Ionization cross sections for Ne^+-Na and Ar^+-Na collisions are measured at the energies of $2-14$ keV using a crossed-beam spectroscopy method. The experimental data and the schematic correlation diagrams are used to analyze and determine the mechanisms for these processes. For the charge-exchange process in Na^+ $-Ar$ collisions two nonadiabatic regions are revealed and mechanisms responsible for these regions are explained. Structural peculiarity on the excitation function for the resonance lines of argon atoms in Na^+ $-Ar$ collisions are observed and the possible mechanisms of this phenomenon are explored. The measured ionization cross sections for Na^+-Ne and Ne^+-Na collisions in conjunction with the Landau-Zener formula are used to determine the coupling matrix element and transition probability in a region of pseudo-crossing of the potential curves.

PACS numbers: 34.80.Dp, 34.70.+e, 34.50.Fa, 32.80.Zb

I. INTRODUCTION

Studies of inelastic processes in slow ion–atom collisions yield extensive data in a quasimolecular mechanism of interaction between the colliding particles. Molecular terms of the system of colliding particles are used in the description of inelastic processes in ion–atom collisions. At present, such terms have been calculated for only a small number of simple systems, so that schematic correlation diagrams for molecular orbitals are widely used but provide only a qualitative explanation of the known features of these processes. However, theoretical calculations alone are insufficient for the complete understanding of the interaction picture due to complicated many–channel character of the processes under investigation. Moreover, because different mechanisms are active at various internuclear distances their study requires several experimental techniques all working together to make a consistent interpretation possible.

On the experimental side, for investigation of the molecular potential curves of a scattering system a set of differential cross sections for various channels following these potential curves are needed. However, due to the limited energy resolution of the differential scattering technique most often is problematic an identification of the specific final states, and only possible a determination of two groups of levels corresponding to one– and two–electron excitation. Thus, in order to infer the differential scattering cross section which results when the system follows specified molecular potential curves on the incoming and outgoing portions of the trajectory, differential energy–loss spectra must be supplemented by cross sections for a photon emission and electron ejection as a function of the respective energies.

Despite many experimental studies of the alkali ion–gas collisions, which have been carried out by various experimental methods [1–23] available data for the absolute cross section for the most inelastic processes are contradictory [1–3, 10, 13] and in some cases unreliable [4].

The inelastic collision mechanism has been studied experimentally and theoretically for the systems Li^+–He and Li^+–Ne in Refs. [8, 9, 18, 24, 25]. Double differential cross sections have also been measured in Ref. [12].

The results of the measurements of the excitation function for Na^+–He and K^+–He colliding pairs in arbitrary units are reported in Refs. [5] and [6]. A relative differential cross section for Na^+–Ar is measured in Ref. [17]. The absolute values of the differential cross section at two fixed energies $E = 200$ eV and $E = 350$ eV of Na^+ ions were determined by using the experimental integral cross sections and the repulsive potential deduced also experimentally are reported in Ref. [11]. Excitation processes in Cs^+–Ar collisions were studied at laboratory collision energies of 0.2–1 keV by means of differential scattering spectroscopy in Ref.[21]. Recently in Ref. [23] a comprehensive study of excitation mechanisms in Na^+–

He and K^+–He collisions at ions energies range of 1.0–1.5 keV by differential scattering spectroscopy was reported. Double differential cross sections were measured by detecting all scattering particles (Na^+, Na, K^+, K, He^+ and He) over a wide range of center-of-mass scattering angles. A systematic study of inelastic processes in K^+–He collisions is presented in Ref. [22]. Absolute cross sections for charge exchange, ionization, stripping, and excitation in K^+–He collisions were measured in the ion energy range 0.7–10 keV.

For Na^+–Ar collisions an energy spectrum of electrons ejected from autoionizing states of Ar atoms at $E = 15$ keV [15] have been briefly reported, but no results exist for lower energy collisions.

The most comprehensive approach to study ion-atom collisions with closed electron shells has so far been carried out only for a Na^+–Ne pair [16]. Though, measurements were performed at a limited energy interval. Therefore, in our study attention will be focused on the extension of the energy interval from 0.7 to 10 keV.

In earlier publication [19] we have reported limited results for inelastic processes realized in Na^+–Ar collisions. In the present study, the differential cross section as well as the energy loss spectrum for Na^+–Ar collisions will be investigated additionally over a wide range of energy and scattering angles.

To our mind the reason for a lack of systematic measurements and reliable data for alkali metal ions and rare gas atoms collisions, and having not at all measurements for inert gas ions collisions with alkali metal atoms are linked with experimental difficulties. Mainly, in the case of the alkali metal ions and rare gas atoms collisions these difficulties related to collections and detections of secondary particles, while, in case of the rare gas ions and alkali metal atoms collisions mostly related to the preparation of alkali metal atoms as a target.

The lack of systematic absolute cross sections measurements for $Na^+ - Ne$ and $Ne^+ - Na$ colliding pairs motivated the present detailed investigation of the primary mechanisms for these collision processes.

The collision of a Na^+ ion beam with Ne and Ar atoms leads mainly to the following processes:

$$\begin{aligned} Na^+ + Ne &\rightarrow Na + Ne^+, && (1)\\ &\rightarrow Na^+ + Ne^+ + e, && (2)\\ &\rightarrow Na^+ + Ne^*, && (3) \end{aligned}$$

and

$$\begin{aligned} Na^+ + Ar &\rightarrow Na + Ar^+, && (4)\\ &\rightarrow Na^+ + Ar^+ + e, && (5)\\ &\rightarrow Na^+ + Ar^*. && (6) \end{aligned}$$

In the charge-exchange processes (1) and (4) the Na atom and Ne^+ or Ar^+ ion can be in the ground states or in different excited states. The reactions (2) and (5) represent the ionization processes for the target atoms, that include different channels for the excitation of the Na^+ ion or/and $Ne^+(Ar^+)$ ion, as well as the excitation of autoionization states of the target atom that leads to its ionization. The excitation processes (3) and (6) include different channels for excitation of the Na^+ ion or/and Ne(Ar) atom.

In collisions of Ne^+ and Ar^+ ions with a Na atom let's consider only charge-exchange and ionization processes:

$$\begin{aligned} Ne^+ + Na &\rightarrow Ne + Na^+, && (7)\\ &\rightarrow Ne^+ + Na^+ + e && (8) \end{aligned}$$

$$\begin{aligned} Ar^+ + Na &\rightarrow Ar + Na^+, && (9)\\ &\rightarrow Ar^+ + Na^+ + e, && (10) \end{aligned}$$

The processes (7) and (9) represent the charge-exchange reactions when the Ne(Ar) atom and Na^+ ion can be in the ground state or in different excited states, while a result of the ionization reactions (8)

and (10) includes different channels for the excitation of the Na^+ ion or/and $Ne^+(Ar^+)$ ion, as well as excitation of autoionization states of the target atom that leads to its ionization.

The simultaneous study of the processes (1) and (7), as well as (4) and (9), when products of the reactions are in the ground states represent a fundamental interest because they are the reversible processes. A symmetry of these processes arises from the concept of time reversal. The symmetry transformation that changes a physical system with a given sense of the time evolution into another with the opposite sense is called time reversal. The symmetry of these processes means that the probabilities for the processes $Na^+ + Ne \rightarrow Na(g.s.) + Ne^+(g.s.)$ ($g.s.$ hereafter refers as the ground state) and $Na^+ + Ar \rightarrow Na(g.s.) + Ar^+(g.s.)$ are the same as the probabilities for the reversed processes $Ne^+ + Na \rightarrow Ne(g.s.) + Na^+(g.s)$ and $Ar^+ + Na \rightarrow Ar(g.s.) + Na^+(g.s.)$. This reciprocity leads to the important principle of detailed balance that relates the cross section, for example, for the reaction $Na^+ + Ne \rightarrow Na(g.s.) + Ne^+(g.s.)$ with that of the time-reversed reaction $Ne^+ + Na \rightarrow Ne(g.s) + Na^+(g.s.)$. Motivated by the CP violation found in the neutral kaon system [26], several tests of time reversal invariance in low-energy nuclear physics have been performed in the weak, electromagnetic, and strong interactions and were consistent with the time irreversibility [27]. Since an experimental test of the detailed balance and time irreversibility in the reactions $^{27}AI + p \leftrightarrows {}^{24}Mg + \alpha$ [28] this problem still remains essential and important [29]. The detailed balance and time irreversibility have been also studied in kinetics [30]. In our best knowledge there is no studies of time irreversibility and detailed balance in atomic collisions. The above mentioned processes are good candidates for the such test. However, experimental difficulties of identifications of the ground states of the charge-exchange products do not allow us to proceed accurate measurements. Though this task poses challenges, they are challenges we are ready to face.

A simultaneous study of the ionization processes (2) and (8), as well as (5) and (10) also represent a particular interest. A close attention to the reactions (2) and (8), and (5) and (10) shows the similarity of the reactions products. One of the objectives of this work is to show that in some cases (e.g. for $Na^+ - Ne$) the information extracted from the theoretical calculations can be obtained experimentally using a simple approach, namely by measuring a relative ionization cross section for $Na^+ - Ne$ and $Ne^+ - Na$ colliding pairs.

Below we report the absolute total and differential cross sections for charge-exchange, ionization as well as the excitation of the both the projectile and target particles and energy loss spectra in collisions of Na^+ ions with Ne and Ar atoms, and $Ne^+$and Ar^+ ions with a Na atom. In later case, the cross section of ionization will be reported for the first time.

The remainder of this paper is organized in the following way. In Sec. II the experimental set-ups and procedures are described and four different experimental methods of measurements for collision experiments are presented. Here we introduce the procedures for measurements of the absolute total and differential cross sections for charge-exchange, ionization and excitation. Results of measurements for the processes (1)–(3), (4)–(6), (8), and (10), the comparison of our measurements with results of previous experimental studies, and discussion of mechanisms for different processes occurring in Na^+–Ar collision are given in Sec.III. The method and procedure for estimation of some theoretical parameters (transition probability, matrix element) from our experimental results are reported in Sec. IV. Finally, in Sec.V we summarize our investigations and present the conclusions.

II. EXPERIMENTAL SET-UPS AND PROCEDURES

The basic experimental approaches used in the present experiments for measurements of total and differential cross sections of ionization, charge-exchange and excitation processes are the following: crossed-beam spectroscopy method, refined version of a capacitor method, collision and optical spectroscopy methods. The basic experimental set-up for measurements of the total and differential cross sections of ionization, charge-exchange and excitation processes in collisions between Na^+ ion and Ne and Ar atoms was discussed previously in detail in Ref. [22], so the only brief description will be given here. The uniqueness of our experimental approach [22] is that for colliding pairs $Na^+ -$ Ne and $Na^+ -$ Ar involved in the above mentioned processes the quality of the beam as well as the experimental conditions always remain identical because the experimental apparatus has three collision chambers. The latter allows to use a refined version of the capacitor method, collision spectroscopy method, and optical spectroscopy method under the same "umbrella." For the experimental measurements of the ionization cross section

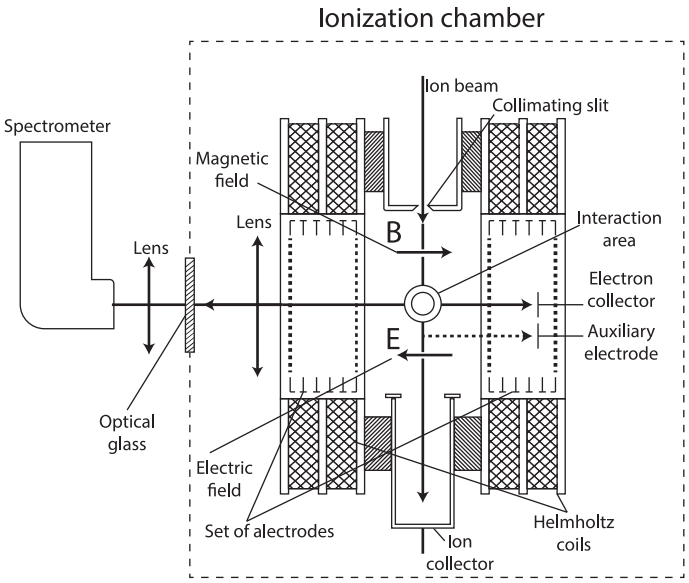

FIG. 1: Schematic diagram of the experimental set-up for study of collisions of ions with alkali metal atoms.

in collisions between Ne^+ and Ar^+ ions and an alkali–metal atom a new experimental set-up is developed using a crossed–beam spectroscopy method. Details of the apparatus and description of the method are presented below.

A. Crossed–beam spectroscopy method

Measurements of the ionization in collision of ions with alkali–metal atoms are related to well known difficulties: preparation of the target; determination of its density; protection of the surface of an ionization chamber and insulators from desorption of a metallic vapor, etc. In the present study, for measurements of the ionization cross section of alkali metal atoms, we are using the method of intersected beams. This method of measurement of the ionization cross section has some advantage compared to other methods. Particularly, in the framework of the method, there is no need to avoid the scattering of an incident beam (as it is peculiar e.g. for a capacitor method) and secondary particles (recoil ions and electrons) on a collector, the emission of electrons from the surface of collectors, etc. The idea of crossed–beam method was suggested in Ref. [31], and used to study the ionization and charge transfer in proton–hydrogen atom collisions. Here this method is significantly elaborated and for the first time is used to investigate the ionization of alkali metal atoms. A schematic drawing of the apparatus for the measurement of the ionization cross section is shown in Fig. 1. The core part of the experimental set-up consists of the ion source, magnetic mass-analyzer, ionization chamber, source of an atomic beam, system for collection of light from the crossing beam region and spectrometer for analyzing of the radiation.

A primary ion beam from a 30 MHz radiofrequency ion source, using permanent longitudinal magnetic field, passes through the single channel capillary formed by the collimating slit and enters into the ionization chamber and is collected by an ion collector. An input of high-frequency power in discharge was carried out by an inductive connection. The power needed to cause the discharge in the ion source was about 150 W. The formation of a plasma pinch in the extraction region is possible by the Pyrex cup and stainless steel capillary. The extraction voltage is 1.0-2.5 keV and the density of the ion beam in the ionization chamber (after passing the magnetic mass–analyzer and collimating slit) is about 0.1 mA/cm^2. A neutral atom beam emerged from an aperture and passed through a collimating slit and directed into the interaction area of the ionization chamber. The atomic beam itself is formed by an extraction nozzle of an oven, where an alkali metal vapor is generated. A diameter of the nozzle is 0.6 mm, while the length of the channel is 6 mm. The oven is made from a tantalum with a massive cone which is screwed on a crucible with the evaporated metal. The heating of the oven is performed by the current

of 1.8–2.0 A. The evaporated metal temperature is measured and controlled by the thermocouple that is mounted on the oven. At the exit from the oven at the distance of 10 mm from the nozzle the density of the sodium atoms beam compose 0.3×10^{11}–3×10^{11} cm^{-3}. The primary ion beam and the modulated atomic beam cross each other perpendicularly at the interaction area of the ionization chamber that is surrounded by magnetic and electric fields. The magnetic field is created by the Helmholtz coils, while the uniform electric field is produced by the set of circular electrodes. Both fields are parallel to each other, opposite directed and perpendicular to the ion and the modulated atomic beams. The atomic beam that is not shown in Fig. 1 is perpendicular to the drawing plane. The magnetic field allows determination of the crossing beam region from where the electrons are collected onto the collector, while the uniform electric field is needed for transporting these electrons towards the electron collector for the registration. Electrons formed in the ionization chamber, as a result of collision of the ionic and atomic beams are collected by the collector of electrons. The electrons, those are produced mostly in the crossing region of the ion and atomic beams, due to the presence of transverse magnetic field can escape from the crossing region just transversely with respect to the direction of the ion beam. The strength of the magnetic field accounts 100-200 Oersted. This means that the shift towards the longitudinal direction does not exceed $1-2$ mm of the Larmor radius, and hence ensures to determine sufficiently reliable the effective length of collection of electrons. The strength of the electric field was chosen to maintain collection of all electrons with the energy up to 23 eV. The last allows to detect electrons from autoionization processes resulting in a liberation of the electrons with the energy of about 20 eV that may be the dominant process in this collision. However, let us mention, that the method allows the collection of electrons with energy up to 45 eV, with the probability close to 90%. A current of electrons on the collector is induced by the electrons produced due to the ionization of the atomic beam and electrons of the "background" induced by the ion impact. For allot of a partial current due to the ionization of "background "atoms, it is possible to carry out a modulation of the atomic beam or to use an auxiliary electrode, implemented in our apparatus. The auxiliary electrode is shifted with respect to the main collector of electrons, therefore for a correct orientation of the atomic beam the detector can collect the electrons formed during interaction of ion beam with the "background" atoms.

For the measurements of the absolute ionization cross section it is needed to know a geometric dimension of the interaction area, an effective length of collected electrons produced in the collision, as well as it is necessary to control a single collision condition, determine the density of particles in the target beam and the flow of incident particles as well. For this reason an optical channel is used that is located on the left side of the ionization chamber. This channel consists of a lens, optical glass and spectrometer with a photoelectron adaptor and photomultiplier that is cooling by liquid nitrogen. The radiation from the beams' crossing region that is produced due to the excitation of colliding particles is extracted and collected perpendicularly to the beams along the axis of Helmholtz coil on a side opposite to the collector of the electrons.

One of the problems, arising during the measurement of the absolute ionization cross section of alkali–metal atoms, as was mentioned above, is related to the determination of the density of the target beam. The method of determination of the sodium atom beam density used in our work is based on the measurement of the intensity of resonant lines of a Na atom excited by a proton impact. We choose this approach for determination of target density because the excitation cross section of the resonance line induced by protons collision belongs to processes which cross sections are measured more reliable [32–34]. A special attention was paid to the reliable determination and monitoring of the absolute spectral sensitivity of the light recording system. This was done by a registration of a Ne atom line ($\lambda = 585.2$ nm, transition $3p\,[1/2]_0 - 3s[1/2]_1$) excited by the proton at an energy of 10 keV. The cross section of this line is known [35], and the wave length of the line sufficiently close to the wave length of resonance lines of a Na doublet. As to the concentration of Ne atoms in the region of collection of the electrons, it could be measured by a simple and reliable method – by measuring the pressure of neon in the collision chamber, using an ionization manometric lamp, calibrated by a compression manometer of Macleod gauge.

The sources of measurement uncertainties of the method are mostly related to the nature of the vapor–metallic target, impossibility of quick shutdown of the target, the increase of surface conductivity of an insulator due to condensation of Na vapor, and the presence of heated elements in the ionization chamber. All these uncertainties were minimized in our measurements. The resultant uncertainty of the measurements is estimated as 15%, and is linked mainly with the measurement of the Ne pressure, the accuracy of which is estimated as 7%.

B. Refined version of a capacitor method

A beam of Na^+ ions from a surface-ionization ion source is accelerated and focused by an ion – optics system, which includes quadruple lenses and collimated slits [22]. After the beam passes through a magnetic mass spectrometer, it enters the collision chamber containing Ne and Ar gases. The pressure in the collision chamber when there is no a Ne or Ar target gas is kept at about 10^{-6} Torr, while the typical pressure under operation is 10^{-4} Torr, which is low enough to ensure single–collision conditions. The charge–exchange and ionization cross sections were measured by a refined version of the capacitor method [36]. In an earlier paper [4] the measurements were performed by the standard transfer electric field method. It is the customary procedure to use one of the central electrodes as the measurements electrode. We consider that such an approach is the reason for significant errors in measurements [4] because scattered primary ions may strike the electrodes used for measurements. To avoid this deficiency we used a refined version of the transfer electric field method by shifting from the central electrode (a standard method) to the first electrode (towards the beam entrance side). In this case the defeat of the electrodes by the scattered primary ions that affects the results of measurements is substantially reduced. Due to fringing effects at the edges of this electrode a system of auxiliary electrodes between the first electrode and the entrance slit were installed. These auxiliary electrodes create a uniform potential near the first electrode. The first electrode, the auxiliary electrodes, and the entrance slit are all positioned together as close as possible. This close arrangement limits the scattering region of the beam to the entrance side. The primary ions are detected by the Faraday cup. The particles (secondary positive ions and free electrons) produced during collision are detected by a collector. The collector consists of two rows of plate electrodes that run parallel to the primary ion beam. A uniform transverse electric field, responsible for the extraction and collection of secondary particles, is created by the potentials applied to the grids. This method yields direct measurements of the cross section σ^+ for the production of singly positively charged ions and σ^- for electrons as the primary beam passes through the gas under study. These measured quantities are related in an obvious way to the capture cross section σ_c and the apparent ionization cross section σ_i and are determined as

$$\sigma^+ = \sigma_c + \sigma_i, \qquad \sigma^- = \sigma_s + \sigma_i. \tag{11}$$

In (11) σ_s is the stripping cross section of the incident ion. The ionization cross section σ_i is always larger than the cross section for stripping σ_s.

For Na^+- Ne collisions, the uncertainty in the measurements of charge–exchange and ionization cross sections are estimated to be 15%. This is determined primarily by the uncertainty in the measurement of the absolute values of the cross sections σ^+ and σ^- and by the uncertainty in the measurement of a target gas pressure in the collision chamber.

For Na^+-Ar collisions, the uncertainty in the measurements of the absolute values of the cross sections σ^+ and σ^- is estimated to be 15% over the entire energy interval studied. This is determined primarily by the uncertainty in the measurement of the target gas pressure in the collision chamber. The uncertainty in the determination of the ionization cross section σ_i, is estimated to be 15% over the energy range and it is determined by the error in the measurement of σ^-. The uncertainty in the measurements of the capture cross sections σ_c at the energy less than 2 keV is estimated to be 15%, while at the energy 5 keV and above the uncertainty does not exceed 25%. For Na^+- Ar collisions at the energy less than 2 keV the cross section σ^+ is significantly larger than σ^-. Accordingly, the error in the determination of the capture cross section σ_c in this energy region is related primarily by the error in the measurement of σ^+. With increasing of the Na^+ beam energy the cross sections σ^+ and σ^- becomes more nearly equal. As a result the error in the determination of σ_c increases.

C. Collision spectroscopy method

The energy–loss spectra and differential scattering experiments have been performed with a collision spectroscopy apparatus. Since the details of the apparatus have been given elsewhere [37], only a brief description will be given below.

The primary beam extracted from the ion source was accelerated to the desired energy before being analyzed according to q/m (q and m are the ion's charge and mass, respectively). The analyzed ion

beam was then allowed to pass through the collision chamber by appropriately adjusting the slits prior to entering into a "box" type electrostatic analyzer. The energy resolution of this analyzer is $\Delta E/E = 1/500$. Automatic adjustments of the analyzer potentials gives the possibility for investigation of the energy–loss spectra in the energy range of 0–100 eV. The differential cross section is measured by rotating the analyzer around the center of collisions over an angular range between 0° and 25°. The laboratory angle is determined with respect to the primary ion beam axis with an accuracy of 0.2°.

For the measurements of the charge–exchange differential cross section the charge component of scattered primary particles realized in the collision chamber is separated by the electric field and neutral particles formed by electron–capture collisions are registered by the secondary electron multiplier. Such a tool gives us the possibility to determine the total cross sections and to compare them with the results obtained by the refined version of the capacitor method [36]. In addition, the measured energy–loss spectrum gives detailed information related to the intensity of inelastic processes realized in the excitation, charge–exchange and ionization processes.

D. Optical spectroscopy method

The method used for the optical measurements have been described previously [38], therefore a brief description will be given here. The alkali metal ion beam leaving the surface–ionization ion source is first accelerated to a predetermined energy. It is then focused by the quadruple lenses and analyzed by the mass spectrometer. The emerging ions passed through a differentially pumped collision chamber containing the target gas at low pressure. The ion current is measured by the collector and the light emitted, as a result of the excitation of colliding particles, from the collision chamber is viewed perpendicularly to the beam by a spectrometer. The spectral analysis of the radiation was performed in the vacuum ultraviolet as well as in the visible spectral regions. The linear polarization of the emission in the visible part of the spectrum is analyzed by the Polaroid and the mica quarter-wave phase plate in front of the entrance slit of the monochromator. The phase plate is placed after the polarizer, is rigidly coupled to it, and used to cancel the polarizing effect of the monochromator. A photomultiplier tube with the cooled cathode is used to analyze and detect the emitted light. The spectroscopic analysis of the emission in the vacuum ultraviolet region is performed with the Seya-Namioka vacuum monochromator, incorporating a toroidal diffraction grating. The radiation was recorded by the secondary electron multiplier used under integrating or pulse-counting conditions. The outputs of the photomultiplier and the secondary electron multiplier were recorded by the electrometers. The polarization of the radiation in the vacuum ultraviolet was not taken into account. The absolute excitation cross sections for the resonance lines of sodium that are determined by comparing the measured output signal with one that due to the excitation of a nitrogen by an electron impact. A particular attention is devoted to the reliable determination and control of the relative and absolute spectral sensitivity of the light–recording system. This was done by measuring the signal due to the emission of molecular bands and atomic lines excited by electrons in collisions with H_2, N_2, O_2, and Ar. For this, an electron gun was placed directly in front of the entrance slit of the collision chamber. The relative spectral sensitivity, and the values of the absolute cross sections, is obtained by comparing the cross sections for the same lines and molecular bands reported in Refs. [39–43]. The uncertainties in the excitation cross sections for the Na^+- Ar system are estimated to be 20% and the uncertainty of the relative measurements does not exceed 5%.

III. EXPERIMENTAL RESULTS AND ANALYSIS

In what follows, the results for Na^+ion collisions with the Ne and Ar atoms and Ne^+ and Ar^+ ions collisions with the alkali metal target atom Na are presented and the findings are compared with data from the literature. The results for the cross section measurements are shown in Figs. 2–6. The energy dependences of the charge–exchange, ionization and excitation for Na^+–Ne and Na^+–Ar collisions are presented in Figs. 2, 3 and 4, respectively. Here for the comparison we also present data of other authors. Results of the first measurement of the energy dependence of ionization cross sections for the processes (8) and (10) are presented in Fig. 5. Fig. 6, where we plot the reduced cross section $\varrho = \theta \sin\theta\sigma(\theta)$ versus reduced angle $\tau = E\theta$, shows the typical example of angular and energy dependences of differential cross sections in the laboratory system when Na^+ ions are scattering on the Ar atoms at a fixed energy $E = 5$

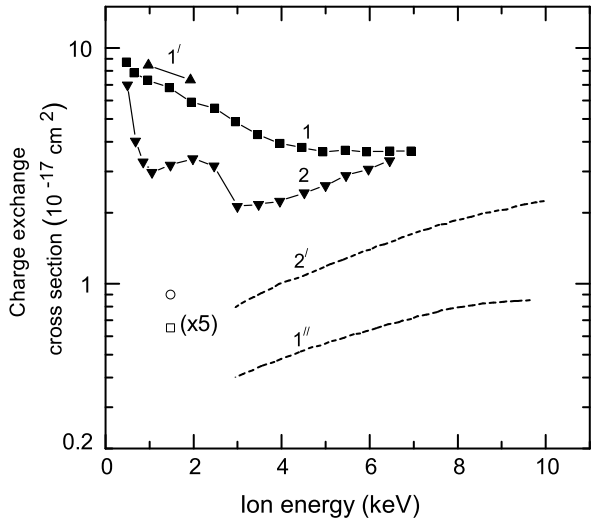

FIG. 2: Dependences of the absolute charge–exchange cross sections on energy of a Na^+ ion in Na^+-Ne and Na^+–Ar collisions. Curves: 1 – Na^+–Ne, present data; 1′ – Na^+-Ne, data from Ref. [16]; 1″ – Na^+-Ne, data from Ref. [4]; 2 – Na^+-Ar, present data; 2′ – Na^+-Ar, data from Ref. [4]; ∘ – Na^+-Ar, electron capture in resonance state, data from Ref. [17]; □ – Na^+-Ar, electron capture with the excitation of target ion, data from Ref. [17] are multiplied by factor of 5.

keV. The reduced scattering angle is defined as $\tau = E\theta$, where E is the energy of the incident beam in keV and θ is a scattering angle in degrees. The filled squires in Fig. 6 represent the elastic scattering of the Na^+ ions, while by the solid circles are shown results of the direct excitation of the Ar atoms in 4p and 3d Rydberg states. In addition, we estimated the electron energies released in Na^+-Ne and Na^+-Ar collisions. The estimates were obtained from the measurements of the dependences of electron current in the measuring electrodes on the potential applied to these electrodes for the collection of electrons. It was found that the energy of the most liberated electrons is below $10 - 15$ eV.

The results for the charge-exchange cross section for Na^+-Ne and Na^+-Ar collisions along with the data from literature are shown in Fig. 2. The comparison of our measurements for the charge–exchange cross section with the results obtained in [16] at two fixed energy $E = 1$ keV and $E = 2$ keV shows excellent agreement. However, a dramatic difference by about 2 orders in the magnitude, as well as in the behavior of the energy dependences are observed, when one compares our results with the results obtained in [4]. The same tendency, but the discrepancy in the magnitude by about 1 order observed when one compares our results for the Na^+-Ar pair with the data from Ref. [4]. Our results for the charge–exchange processes (1), (4) can be compared with the cross sections obtained in Ref. [17] by integrating the differential cross section over the scattering angle for an electron capture and a capture with the excitation of a target ion at energy of $E = 1.5$ keV, which are 9.0×10^{-18} cm^2 and 1.3×10^{-18} cm^2, respectively. This comparison shows that the discrepancy is threefold.

The results for the ionization cross section for Na^+-Ne and Na^+-Ar collisions along with the data of previous measurements are shown in Fig. 3. The comparison of our ionization cross section for the process (5) with the results obtained in [4] shows a satisfactory agreement at low energies but the discrepancy increases for the energies of ions $E > 4$ keV. In principle, a satisfactory agreement is observed for a Na^+-Ne collision between our results and the results from [3], especially in the energy dependence of the cross sections. A rather significant discrepancy is observed if one compares our results with the results reported in Ref. [10]. Within the accuracy of measurements an excellent agreement is observed between

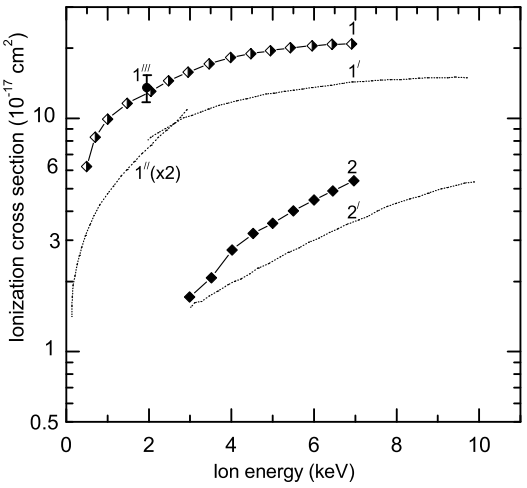

FIG. 3: Dependences of the absolute ionization cross sections on energy of Na^+ ion in Na^+-Ne and Na^+-Ar collisions. Curves: 1 – Na^+-Ne, present data; $1^{'}$ – Na^+-Ne, data from Ref. [3]; $1^{''}$ – Na^+-Ne, data from Ref. [10] are multiplied by a factor of 2; $1^{'''}$ – Na^+-Ne, data from Ref. [16], at fixed $E = 2$ keV; 2 – Na^+-Ar, present data; $2^{'}$ – Na^+–Ar, data from Ref. [4].

our results and the results obtained in Ref. [16] at a fixed ion energy $E = 2$ keV.

The excitation function for Na^+-Ar collisions is presented in Fig. 4. Our data of the excitation function for the resonance lines of sodium (curve 1) and argon atoms (curves 2 and 3) can be compared only with the results obtained in Ref. [17] and only for the collision energy of $E = 1.5$ keV (open circle and open square in Fig. 4). It can be seen from Fig. 4 that the measured total excitation cross sections of a sodium atom in 3p state (curve 1) and argon atom in 4s and $4s^{'}$ states (curves 2 and 3, respectively) are in reasonable agreement with the data obtained in [17].

To the best of the authors' knowledge in the energy range considered there are no experimental measurements of the ionization cross sections for the process of ionization of alkali metal Na by Ne^+ and Ar^+ ions. The first measurements of the absolute ionization cross sections for Ne^+-Na and Ar^+-Na collisions are presented in Fig. 5. As it seen from Fig. 5 the value of the ionization cross section strongly depends on the mass ratio of the colliding particles. In case of Ne^+-Na collisions when the mass ratio of the colliding particles is close to 1, the cross section is larger by a factor of 2 in comparison to the asymmetric case of Ar^+-Na collisions when the mass ratio is greater than 1.

Distinct features are observed in the differential cross section (DCS) as a function of the reduce scattering angle τ shown in Fig. 6. The DCS with the excitation of Ar atoms is smaller than the DCS for the elastic scattering. Another feature is the alternative behavior of the DCS at small angles: the elastic scattering increases at the small angles, while the DCS of the Rydberg states of Ar decreases. The most striking feature is that the ratio of the elastic scattering to the excitation cross sections strongly increases for small values of τ, while for $\tau > 20$ only varies relatively weakly.

The data obtained in this study can be used to make certain conclusions related to possible mechanisms of the investigated processes. To explain these mechanisms one can use a schematic quasimolecular terms for the system of colliding particles. The quasimolecular nature of the interaction of the above considered collision partners can be visually manifested by a representative Na^+- Ar colliding pair. Therefore, below we discuss the mechanisms of the realized processes for this colliding pair. The corresponding schematic correlation diagram constructed based on Bara – Lichten rules [44] is presented in Fig. 7.

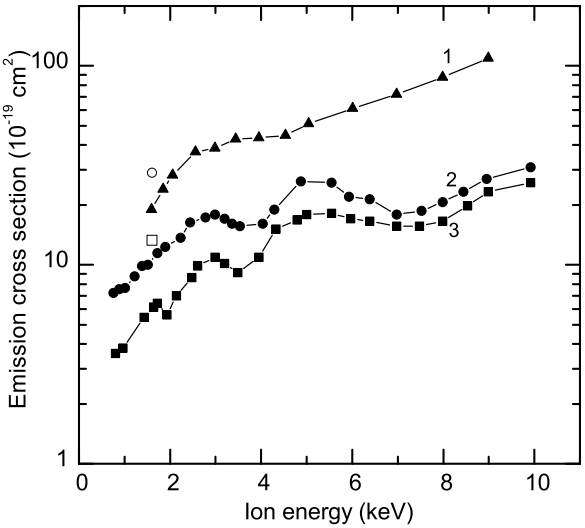

FIG. 4: Excitation function for sodium and argon atomic lines in Na^+-Ar collisions. Curves: 1 – NaI (λ = 389.0 − 389.6 nm, 3p–3s transition); 2 – ArI (λ = 104.8 nm, 4s′–3p transition); 3 – ArI (λ = 106.7 nm, 4s–3p transition); ∘ and □ denote the excitation of sodium and argon atoms, respectively, obtained in Ref. [17].

A. Charge exchange in Na^+-Ar collisions

For determining the processes responsible for the charge exchange in Na^+-Ar collisions, we compare the total charge exchange cross sections (curve 2 in Fig 2.) with the total cross section of radiation for the resonant lines $\lambda = 389.0 - 389.6$ nm of a Na atom (curve 1 in Fig. 4). Taking into account the selection rules and the ratio of the oscillator strengths for these transitions, one can prove that the emission of radiation from any level of the sodium atom culminates in the half of cases in transition of the atom to the resonant state, followed by emission. Consequently, the doubled deexcitation cross section of a Na atom gives a clue related to the capture cross section in the excited state. It can be seen from Fig. 4. (curve 1) that the emission cross section of resonant levels of sodium atoms in Na^+-Ar collisions increases with the increase of the ion energy, amounting to $\backsim 1.8\times10^{-18}$ cm^2 for the ion energy $E = 1.5$ keV and $\backsim 6\times10^{-18}$ cm^2 for $E = 5 - 7$ keV. A comparison of the behavior of the two curves leads to the conclusion that two nonadiabatic regions responsible for an electron capture: one at the energy range $E = 0.5 - 2.0$ keV and the second one – at the energy range $E = 3 - 7$ keV. In the collisions considered here, the electron capture at low energies (up to $E = 2$ keV) takes place as a result of the electron capture into the ground state of a Na atom with the formation of the argon ion in the ground state as well. The process realizes through the channel $Na^+(2p^6)+Ar(3p^6)\rightarrow Na(3s)+Ar^+$ $(3p^5)$, with the energy defect of ΔE = 10.6 eV (one-electron process) and the electron capture into the ground state of the sodium atom with the formation of the argon ion in the excited state, $Na^+(2p^6)+Ar(3p^6)\rightarrow Na(3s)+Ar^+(3p^4$ $(^1D)4s]-29.1$ eV (two-electron process) [17]. This process can occur, as can be seen from the diagram in Fig. 7, as a result of the direct pseudo-crossing of the term corresponding to the state $Na(3s)+Ar^+(3p^5)$ with the ground state of the system $Na^+(2p^6)+Ar(3p^6)$. Since the $Na^+(2p^6)+Ar(3p^6)$ state has only Σ symmetry it follows that the $\Sigma - \Sigma$ transition play a dominant role in the low–energy charge–exchange processes. At the energy range $E > 5$ keV, the electron capture into the excited state Na(3p) of the sodium atom, with the formation of the argon atom in the ground state takes place. This process that is attributed to the reaction $Na^+(2p^6)+Ar(3p^6)\rightarrow Na(3p)+Ar^+(3p^5)$ − 12.7 eV plays the dominating role. The $\Sigma - \Pi$ transitions (see Fig. 7) associated with the rotation of internuclear axis play a certain role in

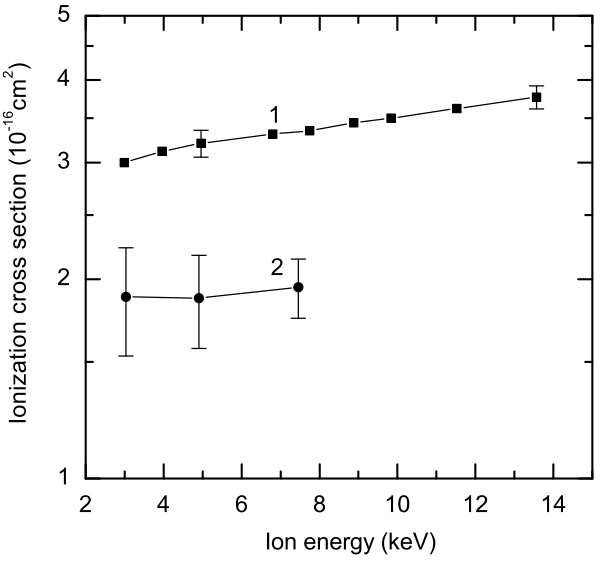

FIG. 5: Dependence of the absolute ionization cross sections on energy of Ne^+ and Ar^+ ions in Ne^+−Na and Ar^+−Na collisions. Curves: 1 – Ne^+−Na; 2 – Ar^+−Na.

the electron capture to the excited 3p states.

B. Ionization in Na^+–Ar collisions

Experiments show that the mechanism of ionization in Na^+–Ar collisions is characterized by the release of predominantly slow electrons with the energies $E < 15$ eV. In order to determine the channel and mechanism of ionization, we estimate the contribution of several inelastic processes that result in emission of slow electrons. To estimate the contribution of direct ionization, we calculated the cross section of this process using the results obtained in [45]. According to [45] in the limit of an united atom, the process of ionization is associated with the emergence of the diabatic energy level to the continuum in the range of the nonadiabatic interaction of molecular orbitals with the same orbital angular momentum. Analysis of correlations of molecular orbitals in the Na^+–Ar system shows (Fig. 7) that the 3p electrons of Ar atom, whose ionization is considered, in the limit of the united atom correspond to the 4d electrons of the Cu^+ ion. Thus, for the estimated cross section we choose the orbital angular momentum $l = 2$. The binding energy E_{nl} of electrons in the nonadiabaticity region was assumed to be equal to the binding energy of 4d electrons of the Cu^+ ion. The effective charge Z_{eff} was determined by the interpolation of the results obtained by Hartree in Ref. [46]. For the 4d electrons of the Cu^+, we obtained $Z_{eff} = 3.1$. The calculation of the direct ionization cross section with these parameters proves that the contribution of this process is less than 1% for the energy of 3 keV of the sodium ions and does not exceed 10% for the energy of 6 keV. The same approach is applied to determine the contribution of electrons yield as a result of stripping of the projectile ions to the measured ionization cross section. As it can be seen from the correlation diagram for the energy level in Fig. 7, the 2p electrons of the Na^+ ion correlate with the 4f electrons of the Cu^+ ion. For this reason, to estimate the cross section we chose the value for the orbital angular momentum $l = 3$ and assumed that $Z_{eff} = 3.1$. In other words, the same as for the 4d electrons of the Cu^+ ion. One also should estimate the contribution of the stripping process. As a result

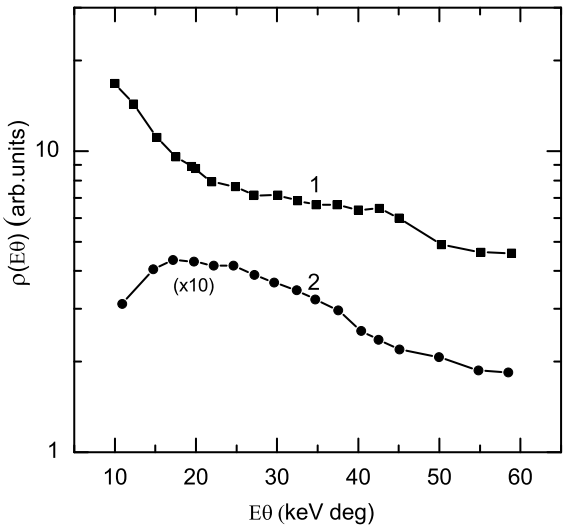

FIG. 6: Differential cross sections for Na^+-Ar collisions as a function of reduced scattering angles at a beam energy $E = 5$ keV. ■ – the DCS of the elastic scattering. • – excitation of the Rydberg states of Ar [$3p^5$ (^{2}P)4p; $3p^5(^2P)3d$]. The later data are multiplied by factor of 10.

of calculation we found that the contribution of stripping to the total electron yield cross sections is 0.1% for an ion energy of 3 keV and less than 4.5% for the ion energy of 6 keV. Consequently, we can conclude that the contribution of these processes to the ionization cross section is insignificant in the entire energy range.

The double ionization of Ar atom and capture accompanied by ionization of Ar ion evidently make a small contribution to the ionization cross section. There are two reasons for this: the absence of pseudo-crossings of the corresponding quasimolecular terms with the ground state term as it seen from diagram in Fig. 7, and the large energy defect for these processes, 43.4 eV and 38.3 eV, respectively.

By comparing consecutively other possible mechanisms of the release of electrons with energy less than $10-15$ eV, we draw the conclusion that the main mechanism of their emergence (along with the contribution of other channels) is associated with the decay of autoionization states in an isolated atom. According to Refs. [15] and [17], these states are those with two excited electrons $Na^+(2p^6)+Ar(4s)\rightarrow Na^+(2p^6)+Ar[3p^4(1D)4s^2; 4p^2]$ −28.7 eV .

C. Excitation processes in Na^+-Ar collisions

Let us consider the excitation mechanisms in Na^+-Ar collisions. The most interesting is exploration of the excitation function in Fig. 4 for the argon atom lines $\lambda = 104.8$ nm and $\lambda = 106.7$ nm for the transitions 4s, 4s′–3p that show oscillatory structures (curve 2 and 3, respectively). It can be seen from the correlation diagram in Fig. 7, the excitation of the Ar(4s) state can occur as a result of i) $\Sigma - \Sigma$ transition between the entrance energy level [$Na^+(2p^6)-Ar$ ($3p^6$)] and the level corresponding to the excitation of the argon atom [$Na^+(2p^6)-Ar$ ($3p^5$4s, 4s′)] or ii) due to the 4p–4s cascade transition in an isolated atom. In the later case the state 4p of the excited argon atom is due to the rotational $\Sigma - \Pi$ transition at small internuclear distances. Indeed, the observed oscillatory structure, a comparatively small cross section $\sigma \sim 10^{-18}$ cm^2, and a large oscillation depth of the curves 2 and 3 in Fig. 4 indicate, according to [47], that namely the contribution of the rotational $\Sigma - \Pi$ transition, with population of the 4p energy level of Ar atom, should be significant in the excitation process. Our results for the differential

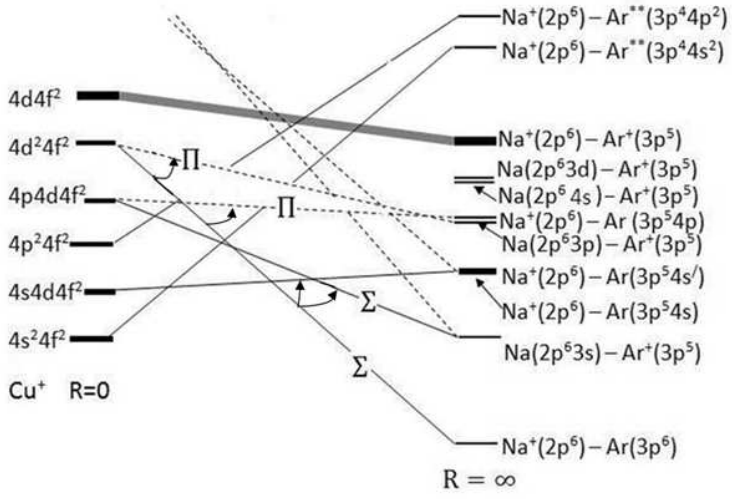

FIG. 7: Schematic correlation diagram for Na^+-Ar colliding pair. Solid lines indicate Σ states, dashed lines indicate Π state.

cross sections presented in Fig. 6 just are the evidence of this fact. Moreover, we have to mention, that among the various channels studied, just the elastic scattering channel and excitation of the Rydberg states 4p and 3d of the argon atom are populated effectively. As to the oscillatory behavior of the data 2 and 3 in Fig. 4, these oscillations are due to the interference of very close quasimolecular states of the $Na^+(2p^5)-Ar$ $(3p^5 4p)$ and $Na(2p^6 3p)-Ar^+(3p^5)$ systems that have the energy scale defect only 0.19 eV. But, if it so, and that is a rule, in accordance with the interference model [48], the energy dependence of the excitation cross section for the $Na(2p^6 3p)$ presented by data 1 in Fig. 4 under the such assumptions may exhibit an oscillatory structure in antiphase that gives the dependence observed for the 4s and $4s^{'}$ lines of the Ar atom. However, the energy dependence of the excitation cross section of the $Na(2p^6 3p)$ atom for the 3p–3s transition with $\lambda = 389.0 - 389.6$ nm in Fig. 4 exhibits only a small structural singularity. This leads to the conclusion, that other channels are contributed to the excitation of the $Na(2p^6 3p)$ state, which can smoothen the oscillatory structure. Therefore, special measures should be taken to explore this irrelevance. It was found, that the flatness of the excitation cross section may occur due to the influence of a cascade transition from the upper sodium levels (e.g. from $4s^2S_{1/2}$ and $3d^2D_{3/2}$) to the sodium 3p level. This assumption was verified indirectly by us from analysis of the ratio of the excitation cross section of the sodium singlet $3p^2P_{1/2}$ and triplet $3p^3P_{3/2}$ states.

It was revealed that the cross section ratio $\sigma(3p^2P_{1/2})/\sigma(3p^2P_{3/2})$ differs from the statistical population in the entire energy range and amounts to ~ 0.7 instead of 0.5. The probabilities of the cascade electron transitions from sodium $4s^2S_{1/2}$ and $3d^2D_{3/2}$ levels to the 3p level of sodium atom are such that the transition from the $4s^2S_{1/2}$ level to the singlet, as well as to the triplet states, is the same and changes the statistical population just insignificantly. However, the transition from the $3d^2D_{3/2}$ level to the sodium singlet 3p level is five times higher compare to the triplet level and, hence, increases the statistical population significantly. Accordingly, from our estimation, and by taken into consideration that the excitation function for the sodium 4s and 3p states are the same (this is a relevant because of the defect $\backsim 0.4$ eV) we can conclude that the absence of a clearly manifested oscillatory structure on the excitation cross section of the Na atom lines can be associated with the effect of the cascade transition from the upper levels.

As to the origin of oscillation, observed on an excitation function for the Ar(4s, $4s^{'}$), to our mind it is caused not by the direct excitation of the 4s and $4s^{'}$ states of the argon atom. The excitation of argon atom takes place into the 4p state and than from here, through the 4p−4s cascade transition it become apparent in the excitation of the 4s and $4s^{'}$ states.

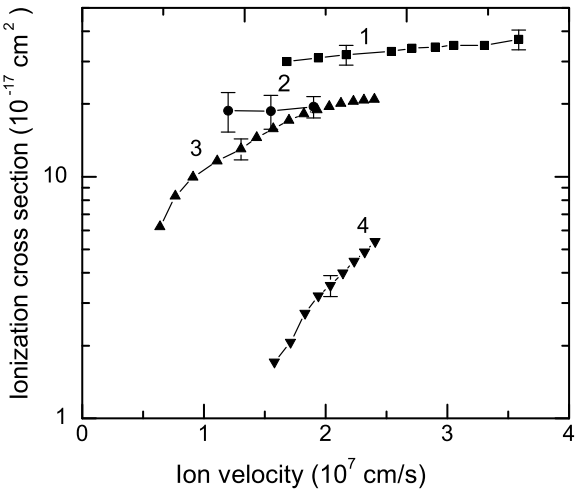

FIG. 8: Velocity dependences of the ionization cross sections for the $(NaNe)^+$ and $(NaAr)^+$ systems. The result of the measurements of the ionization cross section are presented for the following collisions: curve 1 – Ne^+-Na; curve 2 – Ar^+-Na; curve 3 – Na^+-Ne; curve 4 – Na^+-Ar.

IV. DETERMINATION OF THE TRANSITION PROBABILITIES BETWEEN POTENTIAL CURVES OF QUASIMOLECULAR SYSTEM

Let us compare the ionization processes (2), (5), (8) and (10). The velocity dependence of the ionization cross sections for Na^+-Ne, Na^+-Ar, Ne^+-Na and Ar^+-Na collisions are presented in Fig. 8. As is seen from Fig. 8 the magnitude of ionization cross sections strongly depends on the ionization energy of the target atom. The ionization energy of Na, Ar and Ne atoms are 4.8 eV, 15.7 eV, and 20.2 eV, respectively. The lesser the target atom's ionization energy, the bigger is the value of the cross section. This fact is illustrated by the comparison of curves 1 and 3, and 2 and 4, in Fig. 8.

The excitation processes for Na^+-Ne collisions are qualitatively interpreted by the electron promotion model in Refs. [16, 49]. In order to discuss quantitatively the excitation mechanisms, one has to evaluate the crossing parameters by collision experiments or *ab initio* calculations. Unfortunately, the accuracy of the calculations is still not sufficient for many-electron systems. One of the objectives of this work is to show that in some cases (e.g. for Na^+-Ne) the information extracted from a theoretical calculation (e.g. the coupling matrix element) can be obtained experimentally using a simple approach, namely by measuring the ionization cross section of Na^+-Ne and Ne^+-Na colliding pairs in a sufficient energy region.

Usually for determination of transition probabilities for quasimolecular systems in a region of pseudo–crossing of the potential curves one measures the cross section of an inelastic transition between the states, corresponding to these potential curves. What will be shown below, in some cases this probability can be determined, not through a measurement of the cross section for a transition from one channel to the other, but using two independent measurements: the transition from one and, independently, from other channels to a third channel. In this case, for determination of the transition probability it is fully sufficient to determine not the absolute value of cross sections, but only their relation.

Let us consider this method of determination of the transition probability between potential curves, corresponding to the ground state (potential curve X in Fig. 9) and the states, in which particles are charge-transferred (potential curve A in Fig. 9) for the system $(NaNe)^+$. As the third channel, in which

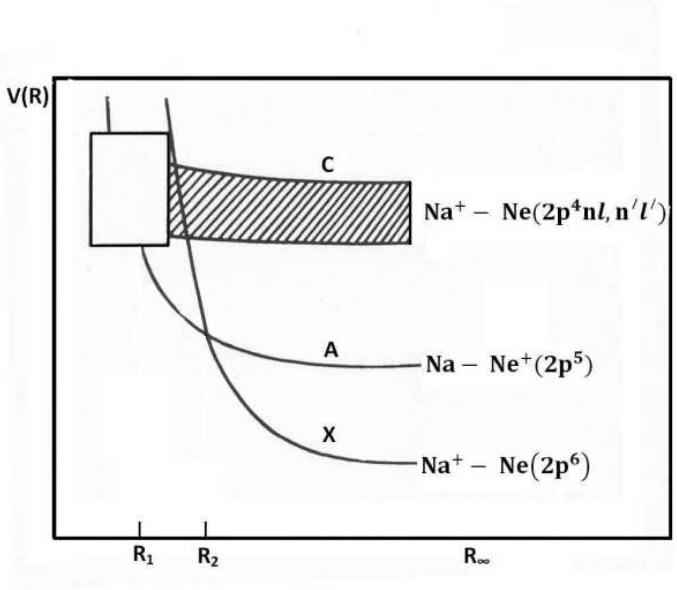

FIG. 9: Schematic presentation of the potential terms for determination of the transition probability and coupling matrix element for $(NaNe)^+$ system. "X" is the entrance potential curve. "A" denotes the potential curve that corresponds to the charge exchange process. "C" represents a band of terms corresponding to autoionization states.

the transition from these two states occurs in considering collisions, can be chosen a channel of atomic autoionization terms (band autoionization states C in Fig. 9). In accordance of choosing of the third channel, it is necessary to have the cross sections for the ionization in Na^+-Ne and Ne^+-Na collisions at the same collision velocity. Such data are obtained in this study. The measurements of the ionization cross sections for the processes (2) and (8) are brought specially to be realized the considered method.

In Ref. [16] it was shown, that the ionization in collision of Na^+-Ne is realized as a result of the sequence transitions, at first due to a pseudo–crossing of the potential curves X and A in the area of R_2 and then by the potential curve A with the band of curves C in the area R_1 as is shown in Fig. 9. In this case, as it easy to see, the mechanism of ionization in Na^+-Ne collision is the same, as in Ne^+-Na collision. The difference in the cross sections of ionization for these pairs are related to the way the system approaches to the pseudo–crossing region: in one case, by the potential curve X, while in the other case, along the potential curve A. Take this fact into the consideration, in a framework of an impact parameter approach, the cross section of ionization in collisions of Na^+-Ne and Ne^+-Na pairs, at the same velocity of relative motion, can be presented, as

$$\sigma_1 = 2\pi(1 - P_0) \int P_{AC}(b) b db, \tag{12}$$

$$\sigma_2 = 2\pi P_0 \int P_{AC}(b) b db, \tag{13}$$

where P_{AC} is the transition probability at the pseudo–crossing of the potential curve A with the band C in the area of R_1 and P_0 is the transition probability between the potential curves X and A in the area of R_2, at the some value of the impact parameter b from the region $b \leq R_1$. The later condition is clear because if this will be not satisfied, particles never reach the region of R_1 and the ionization will not be realized. The transition probability P_0 in the expressions (12) and (13) for the cross sections should be under the integral because it is the function of the impact parameter – $P_0(b)$. However, since location of non-adiabatic area is such that $R_1 < R_2$, the dependence of $P_0(b)$ on the impact parameter b for $b \leq R_1$ is weak and therefore it is physically reasonable to consider $P_0(b) = P_0$ and pull out from

the integral. Since the dependence of the probability P_0 on the impact parameter b is linked to the radial velocity in the transition region, it is possible to estimate a value of the radial velocity sufficiently precisely, corresponding to these probabilities.

From the comparison of the ionization cross sections for Na^+–Ne and Ne^+–Na collisions is obtained that in collision of $(NaNe)^+$ at the energy 7.0 keV, probability $P_0 = 0.62$. To this value of P_0, for the values of R_1 and R_2 from the article [16], corresponds the radial velocity $V_R = 0.7v_0$, where v_0 is the velocity of relative motion of the colliding particles. Now by knowing the transition probability and behavior of the potential curves in a non-adiabatic region one can find the coupling matrix element H_{XA} for nonadiabatic states using the Landau-Zener formula [50, 51] for the probability of a nonadiabatic transition for the pseudo–crossing potential curves

$$P_0 = \exp\left(2\pi \left|H_{XA}\right|^2 / V_R \left|\Delta F\right|\right). \tag{14}$$

In Eq. (14) ΔF is the difference of slopes of the intersecting potential curves. Taking the difference of the slopes ΔF =3 a.u. from Ref. [16], for the coupling matrix element H_{XA} one gets $H_{XA} = 0.14$ a.u. which significantly clarifies the theoretical estimation of the value of this matrix element $H_{XA} = 0.04 - 0.1$ a.u. obtained in Ref. [16]. Despite its limitations, the Landau-Zener formula remains an important tool for a nonadiabatic transition. Even in systems for which accurate calculations are possible, application of the Landau-Zener formula can provide useful estimates of nonadiabatic transition probabilities. Alternatively, if the nonadiabatic transition probabilities and slopes are known, this equation offer a feasible way to obtain the coupling matrix element.

V. SUMMARY AND CONCLUSIONS

In this work, we report the results of the experimental study of inelastic processes realized in collisions of Na^+ ion with Ne and Ar atoms and Ne^+ and Ar^+ ions with Na atoms in the impact energy range $0.5 - 14$ keV. In case of Na^+ ion Ne, Ar atoms collisions the absolute value of the ionization, charge-exchange and excitation cross section are measured at the energy range of $0.5 - 10$ keV, while in the case of Ne^+ and Ar^+ ion collision with Na the ionization cross section is measured at the energy range of $2 - 14$ keV.

Using the experimental set-up based on the crossed-beam spectroscopy method and the unique experimental set-up that includes a refined version of the capacitor method, collision spectroscopy and optical spectroscopy methods of measurements under the same umbrella, and a well–checked calibration procedure of the light recording system, we have measured the absolute values of the charge-exchange, ionization and excitation cross sections for $(NaNe)^+$ and $(NaAr)^+$ systems. The correlation diagram of the $(NaAr)^+$ system has been employed to discuss the mechanism realized in $Na^+ - Ar$ collisions.

For the charge–exchange processes two nonadiabatic regions was revealed in $Na^+ - Ar$ collisions. One region is at low energy, $E < 2$ keV, where the charge–exchange realizes as a result of electron capture into the ground state of the sodium atom with the formation of the argon atom in the ground state also in the region of pseudo-crossing of the potential curves of $^1\Sigma$ symmetry. While the other one is in the energy region $E >3$ keV, where the electron capture into the excited 3p state of a sodium atom takes place and the formation of an argon ion in the ground state plays a dominant role. In this case the $\Sigma - \Pi$ transition is realized and it is associated with the rotation of the internuclear axis.

A primary ionization mechanism for $Na^+ - Ar$ colliding pair is related to the liberation of slow electrons with the energy of $10 - 15$ eV and is associated with the decay of autoionization states in an isolated atom.

The oscillatory behavior of the energy dependence of the excitation cross section of argon atoms is revealed in Na^+–Ar collisions and found that, this excitation is a result of the $\Sigma - \Pi$ transition between the entrance energy level and the level corresponding to the excitation of Ar atoms, and also due to the 4p–4s cascade transition in the isolated atom.

Experimentally measured ionization cross sections, for $Na^+ - Ne$ and $Ne^+ - Na$ colliding pairs in conjunction with the Landau-Zener formula, allow us to determine the coupling matrix element and transition probability in a region of pseudo-crossing of the potential curves.

Acknowledgements

This work was supported by the Georgian National Science Foundation under the Grant No.31/29 (Reference No. Fr/219/6-195/12). R.Ya.K. and R.A.L gratefully acknowledge support from the International Reserch Travel Award Program of the American Physical Society, USA.

[1] J. P. Mouzon, Phys. Rev. **41**, 605 (1932).
[2] D. E. Moe and O. H. Petsch, Phys. Rev. **110**, 1358 (1958).
[3] I. P. Flaks, B. I. Kikiani, and G. N. Ogurtsov, Tech. Phys. **10**, 1590 (1966).
[4] G. N. Ogurtsov and B. I. Kikiani, Tech. Phys. **11**, 362 (1966).
[5] V. B. Matveev, S. V. Babashev, and V. M. Dukelski, Sov. Phys. JETP **28**, 404 (1969).
[6] V. B. Matveev and S. V. Babashev, Sov. Phys. JETP **30**, 829 (1970).
[7] V. V. Afrosimov, S. V. Bobashev, Yu.S. Gordeev, and V. M. Lavrov, Sov. Phys. JETP **35**, 34 (1972).
[8] R. Francois, D. Dhuicq, and M. Barat, J. Phys. B: At. Mol. Phys. **5,** 963 (1972).
[9] D. C. Lorents and G. M. Conklin J. Phys. B: At. Mol. Phys. **5,** 950 (1972).
[10] Z. Z. Latypov, A.A. Shaporenko, Sov. Physics JETP, **42**, 986 (1976).
[11] S. Kita, K. Noda, and H. Inouye, J. Chem. Phys. **63**, 4930 (1975).
[12] V. V. Afrosimov , Yu .S. Gordeev, and V. M. Lavrov Sov. Phys. JETP **41**, 860 (1976).
[13] Yu. F. Bidin and S. S. Godakov, Sov. Phys. JETP Lett. **23**, 518 (1976).
[14] R. Hegerberg, T. Stefensson, and M. T. Elfort, J. Phys. B **11**, 133 (1978).
[15] K. Jrgensen, N. Andersen, and J. Olsen, J. Phys. B **11**, 3951 (1978).
[16] J. O. Olsen, T. Andersen, M. Barat et al., Phys. Rev. A **19**, 1457 (1979).
[17] S. Kita, T. Hasegawa, H. Tanuma, and N. Shimakura, Phys. Rev. A **52**, 2070 (1995).
[18] S. Kita, S. Gotoh, N. Shimakura, and S. Koseki, Phys. Rev. 62, 032704 (2000).
[19] R. A. Lomsadze, M. R. Gochitashvili, R. V. Kvizhinadze, N. O. Mosulishvili, and S. V. Bobashev, Tech. Phys. **52**, 1506 (2007).
[20] S. Kita, S. Gotoh, T. Tanaka et al., J. Phys. Soc. Jpn. **76**, 044301 (2007).
[21] S. Kita, T. Hatada, and H. Inoue, Y. Shiraishi, and N. Shimakura J. Phys. Soc. Jpn. **82**, 124301 (2013).
[22] R. A. Lomsadze, M. R. Gochitashvili, R. Ya. Kezerashvili, N. O. Mosulishvili, and R. Phaneuf, Phys. Rev. A **87**, 042710 (2013).
[23] S. Kita, T. Hattori, and N. Shimakura, J. Phys. Soc. Jpn **84**, 014301 (2015).
[24] B. R. Junker and J C Browne, Phys. Rev. A **10,** 2078 (1974).
[25] V. Sidis, N. Stolterfoht, and M. Barat, J. Phys. B: At. Mol. Phys. **10,** 2815 (1977).
[26] C. R. Christenson et al., Phys. Rev. Lett. **13**, 138 (1964).
[27] E. M. Henley, Annu. Rev. Nucl. Sci. **19**, 367 (1969).
[28] E. Blanke, H. Driller, W. Glockle, H. Genz, A. Richter, and G. Schrieder, Phys. Rev. Lett. **51**, 355 (1983).
[29] A. A. Temerbayev and Yu. N. Uzikov, Phys. Atomic Nucl., 2015, **78** (2015).
[30] R. A. Alberty, J. Chem. Educ. **81**, 1206 (2004).
[31] W. L. Fite, R. F. Stebbings, D.G. Hummer, and R.T. Brackmann, Phys. Rev. **119**, 663. (1960).
[32] V. M. Lavrov, R. A. Lomsadze, Abstracts of XIII ICPEAC , W. Berlin, p. 610, (1983).
[33] R. Shingel and B. H. Branaden, J. Phys. B **20**, L127 (1987).
[34] K. Igenbergs, J. Schweinzer, I. Bray, D. Bridi, and F. Aumayr, Atomic Data and Nuclear Data Tables **94**, 981–1014 (2008).
[35] F. J. De Heer and T. van Eck, Proc. of III ICPEAC, London, p.653, (1963).
[36] B. I. Kikiani, R. A. Lomsadze, and N. O. Mosulishvili et al., Tech. Phys. **30**, 934 (1985).
[37] M. R. Gochitashvili, R. A. Lomsadze et al., Georgian Electron. Sci. J.: Phys. **39**-2, (2004).
[38] M. R. Gochitashvili, N. Jaliashvili, R. V. Kvizhinadze, and B. I. Kikiani, J. Phys. B **28**, 2453 (1995).
[39] J. M. Ajello and B. Franklin, J. Chem. Phys. **82**, 2519 (1985).
[40] S. V. Avakyan, R.N. Ii'In, V.M. Lavrov, G.N. Ogurtsov, Collision processes and excitation of UV emission from planetary atmospheric gases: a handbook of cross sections, 1999 - books.google.com
[41] E. J. Stone and E. C. Zipf, J. Chem. Phys. **56**, 4646 (1972).
[42] K. H. Tan, F. C. Donaldson, and J. W. McConkey, Can. J. Phys. **52**, 786 (1974).
[43] K. H. Tan and J. W. McConkey, Phys. Rev. A **10**, 1212 (1974).
[44] M. Barat and W. Lichten, Phys. Rev. A **6**, 211 (1972).
[45] E. A. Solov'ev, Sov. Phys., JETP **54**, 893 (1981).
[46] R. D. Hartree, The Calculation of Atomic Strictures, Wiley, New York, 1957.
[47] S. V. Bobashev and V. A. Kharchenko, Sov. Phys. JETP, **44**, (1976).
[48] V. H. Ankudinov, S. V. Bobashev, and V. I. Perel, Sov. Phys. JETP **33**, 490 (1971).

[49] U. Fano and W. Lichten, Phys. Rev. Lett. **14**, 627 (1965).
[50] L. D. Landau, Phys. Z. **2**, 46 (1932).
[51] C. Zener, Proc. R. Soc. London A **137**, 696 (1932).